3

Materials and Methods

The present investigation on the thesis entitled "**Corrosion Inhibition and Adsorption Potential of Biomass Extracts-Leaves and Flowers of *Heliconia rostrata and Canna indica* on Corrosion of Mild Steel/Aluminium 1100 in 1 M HCl**" consisted of the following steps.

Phase I: Selection of metal samples and acid medium, Selection of inhibitors and Characterization of inhibitors using UV, FT-IR, HPTLC and GC-MS techniques.

Phase II: Methods adopted: Electrochemical measurements and mass loss methods.

Phase III: Surface analytical techniques.

Phase IV: Quantum chemical studies using Mopac software.

In the present investigation, leaves and flower extracts of ***Heliconia rostrata* (HR) *and Canna indica* (CI)** are selected as inhibitors for Mild steel / Aluminium 1100 corrosion in 1 M HCl. Phytochemical screening of the selected plant extracts were carried out using standard procedure **(Harbone,1973).**

3.1 Phase I: Selection of Metal samples and acid Medium, Selection of inhibitors and Characterisation of inhibitors

3.1.1 Selection of Metals

Mild Steel

Mild steel is a significant material and is widely used in many industries due to its excellence mechanical property, easy availability and low cost. It has been extensively used under different conditions in chemical and allied industries in handling alkalis, acids and salt solutions. Since it suffers severe corrosion in aggressive environment, it has to be protected. A large sheet of cold rolled mild steel coupons with a chemical composition of carbon 0.081%, manganese 0.198%, silicon 0.009%, phosphorus 0.012%, sulphur 0.017%, chromium 0.022%, molybdenum 0.026%, nickel 0.016% and iron 99.62% was utilized for the present study (Figure 3.1).

Aluminium

Aluminium and aluminium alloys have high technological value and wide range of industrial applications due to its outstanding characteristics such as high mechanical

strength, excellent ductility, low density, and good electrical and thermal conductivity. However aluminium and its alloys are reactive materials and are prone to corrosion. Aggressive anions like Cl^- lead to increased corrosion rates of aluminium which brings pitting corrosion.

Aluminium Alloy 1100(AA 1100) with the following composition- Copper 0.05 - 0.2%, Manganese 0.05% , Silicon + Iron 0.95%, Zinc 0.01 %, Aluminium 99% were used for the entire study (Figure 3.1)

The mild steel and aluminium samples, with an active surface of 1cm x 5 cm were used for mass loss measurements and 1cm × 1cm specimen for electrochemical measurements. The samples were mechanically polished, degreased, washed in double distilled water and dried in warm air. Mass loss experiments and electrochemical measurements were done according to **ASTM G1-03**.

Figure: 3 .1 Chemical composition of metal specimen

3.1.2 Selection of Medium

Acid pickling is a method of removing mill scale and rust from iron and steel. Hydrochloric acid and sulphuric acid are widely used as pickling agent for the removal of rust and scale in several industrial processes like cleaning of boilers and heat exchangers. Due to shorter pickling time, HCl is predominantly used than H_2SO_4 in acid pickling process. Hence 1 M HCl was selected for the present study to investigate the inhibitive effect of HR/CI extracts on the corrosion of mild steel and aluminium. 1 M HCl solution was prepared from analytical grade reagents and de-ionized water was used for preparing the solution.

3.1.3 Selection of the Inhibitor

The use of inhibitors is one of the most practical methods for protection against corrosion, especially in acidic media. Numerous inhibitors have been tested and applied industrially as corrosion inhibitors. But they are toxic and expensive. Due to increasing ecological awareness and strict environmental regulations, attention has been now focused towards sustainable, nontoxic and eco-friendly inhibitor for zero environmental impact. The plant raw material contains a wide range of organic compounds and potentially capable of inhibiting corrosion processes on metals. Plant extracts are biodegradable and constitute incredibly rich source of natural chemical compounds that can be extracted by simple procedures at low cost expenses.

The use of natural products otherwise tagged "green corrosion inhibitors" was advocated because it is

- ✓ Inexpensive.
- ✓ Non toxic nature.
- ✓ Environmentally acceptable.
- ✓ Renewable source.
- ✓ Readily available.

Plant extracts are incredibly rich sources of naturally synthesized chemical compounds (*e.g.* amino and organic acids, glycosides, alkaloids, polyphenols, steroids, flavonoids and tannins) and most are known to have inhibitive action.**(Fouda *et al,*2012).**For the present study, leaves and flower extracts of ***Heliconia rostrata* (HR) *and Canna indica* (CI)** were used as corrosion inhibitors for mild steel and aluminium surface in 1 M HCl.

3.1.4 Preparation of inhibitor

***Heliconia rostrata* leaves and flowers (HRL, HRF) *and Canna indica* leaves and flowers (CIL, CIF)** were collected in and around Coimbatore and shade dried. The selected plants were authenticated by Botanical Survey of India (BSI/SRC/5/23/2015/Tech-527, 972) Coimbatore, Tamilnadu. The extract was prepared by refluxing 25 g of powdered plant leaves and flower in 1 M HCl for 3 h and kept overnight for cooling. The cooled extracts were filtered and made up to 500 ml with 1 M HCl to get 5% extract of the inhibitor.

3.1.5 Characterization of HR/CI Extracts

3.1.5.1 Phytochemical screening Test

Phytochemical examinations were carried out for all the extracts (leaves and flower of HR/CI) as per the standard procedures mentioned.(**Harborne, 1973**) **(Appendix I).**

3.1.5.2 UV-Visible spectra:

The UV-Vis spectra give basic information about the structure of the molecule. Absorption of UV and visible light involves promotion of the electrons in the σ and π orbital from the ground state to higher energy states. Investigated plants HR/CI were subjected to UV-VIS Spectrophotometric characterization over 200-600nm using **PC based double beam spectrophotometer 2202**.

3.1.5.3 FT-IR

FT-IR spectroscopy is used to identify the functional groups present in the extracts. To find out the functional groups present in the HR/CI extracts FT-IR study has been conducted. The sample for FT-IR studies were prepared by finely mixing the extract with spectroscopically pure KBr and then pressed by using a die so as to get a fine transparent pellet. The FT-IR spectrum was recorded for leaves and flowers of HR/CI extracts with a frequency ranging from 4000 to 400 cm^{-1} using Perkin Elmer FT-IR spectrophotometer with the SOFTWARE – OPUS version 6.5.

3.1.5.4 HPTLC

In order to examine the presence of terpenoids, Coumarins and Flavonoids the ethanol distillate of 25 mg of dried of plant sample (HRL, HRF) was weighed accurately in an electronic balance (Afcoset) and dissolved in 250µl of Ethanol and centrifuged at 3000 rpm for 5 minutes. The solution was used as test solution for HPTLC analysis.

Sample application

2 µl of test solutions and 2 µl of standard solution were loaded as 5mm band length in 4 x 10 Silica gel $60F_{254}$ TLC plate using Hamilton syringe and CAMAG LINOMAT 5 instrument.

Spot development

The samples loaded plate was kept in TLC twin trough developing chamber (after saturated with Solvent vapour) with respective mobile phase (Terpenoid, Flavonoid and Coumarin) and the plate was developed up to 90mm.

Photo-documentation

The developed plate was dried by hot air to evaporate solvents from the plate. The plate was kept in Photo-documentation chamber (CAMAG REPROSTAR 3) and captured the images at Visible light, UV 254nm and UV 366nm.

Derivatization

The developed plate was sprayed with respective spray reagent (Terpenoid, Flavonoid and Coumarin) and dried at 100°C in Hot air oven. The plate was photo-documented in Visible light mode using Photo-documentation (CAMAG REPROSTAR 3) chamber.

Scanning

After derivatization, the plate was fixed in scanner stage (CAMAG TLC SCANNER 3) and scanning was done at 500 nm. The Peak table, Peak display and Peak densitogram were noted. The software used was winCATS 1.3.4 version.

3.1.5.5 GC- MS Analysis

GC analysis separates all the components in a sample and provides a representative spectral output. The chemical composition of the leaves and flowers of HR/CI were characterized by use of gas chromatography and mass spectrometry (GC-MS).

In order to identify the individual compounds in the ethanol distillate of leaves and flowers of HR/CI extracts, GC-MS technique was used **(Seng *et al*, 2006)**. The GC-MS instrument was Fisons 800 Top GC coupled to Fisons MD 800 series MS quadrupole mass detector. The aqueous distillate was desorbed in GC injector at 100˚C for 2 minutes in split less mode and chromatographic separation was carried out on a 30 m × 0.25 mm × 0.25 µm film thickness DB-5MS (5 % phenyl - 95 % methyl polysiloxane) capillary column. The GC oven temperature was programmed from 100˚C (held for 1 min.) to 250˚C at a rate of 6˚C. Helium was used as a carrier gas at a constant flow of 1.0 mL/min. Mass spectra was recorded in electron impact mode at 70 eV, scanning the 20 - 550 m/z range. The interface and source temperature were 200˚C and 250˚C, respectively. All analyses were carried out in duplicate.

3.2 Methods adopted

3.2.1 Electrochemical Methods

Electrochemical studies were carried out using conventional three electrode cell with platinum foil as counter electrode, saturated calomel electrode (SCE) as reference electrode and MS/AA 1100 specimen of 1 cm^2 area as working electrode. Biologic system interfaced with an IBM computer and EC lab 10.4 software was used for data acquisition and analysis. The experiments were carried out for 30 minutes of immersion period at room temperature.The following techniques were carried out.

- ✶ Potentiodynamic Polarisation Method.
- ✶ Linear Polarisation Resistance Method.
- ✶ Electrochemical Impedance Spectroscopic Techniques.

3.2.1.1 Potentiodynamic Polarization Method (Tafel Polarisation)

Polarization technique was carried out using EC lab software from a cathodic potential of -0.1 V to an anodic potential of -1 V with respect to corrosion potential at a sweep rate of 2 mVs^{-1}.The values of corrosion potential (E_{corr}), corrosion current density (I_{corr}) anodic and cathodic Tafel slopes (b_a and b_c) can be evaluated from the anodic and cathodic region of Tafel plots. The linear Tafel segments of anodic and cathodic curves were extrapolated to corrosion potential to obtain corrosion current densities (I_{corr}). For Tafel polarization method, the corrosion inhibition efficiency (I.E. %) was evaluated from the measured I_{corr} values using the relationship. (**Abdel Rehim *et al,* 2001**)

$$\text{Inhibition efficiency (\%)} = \frac{I_{corr(blank)} - I_{corr(inh)}}{I_{corr(blank)}} \times 100 \qquad \textbf{(3.1)}$$

where, $I_{corr\ (blank)}$ = corrosion current in the absence of inhibitor.

$I_{corr\ (inh)}$ = corrosion current in the presence of inhibitor.

3.2.1.2 Linear polarisation resistance method

Linear polarisation study was carried out from -0.02V Vs OCP at the scan rate of 0.125 mV s^{-1}

Polarization resistance values were determined from the slope of the potential current lines,

$$R_p = A\frac{dE}{di} \qquad \textbf{(3.2)}$$

Where A is the surface area of the electrode, dE is change in potential and di is the change in current. The Rp values were used to calculate the inhibition efficiencies (IE %) using the relationship, (**Outirite *et al*, 2010**)

$$\text{Inhibition efficiency (\%)} = \frac{R_{p(inh)} - R_{p(blank)}}{R_{p(inh)}} \times 100 \qquad \textbf{(3.3)}$$

Where, $R_{p\ (inh)}$ = polarization resistance in the presence of inhibitor.

$R_{p\ (blank)}$ = polarization resistance in the absence of inhibitor.

3.2.1.3 Electrochemical impedance spectroscopic technique

Electrochemical impedance measurements were carried over the frequency 20 kHz to 0.1Hz at open circuit potential.

The values of (R_t+R_s) correspond to the point where the plot cuts Z' axis at low frequency and R_s corresponds to the point where the plot cuts Z' axis at high frequency. The difference between R_t and R_s gives the charge transfer resistance (R_{ct}) values. The Cdl values were obtained from the relationship **(Macdonald,1987)**.

$$\mathbf{C_{dl}} = \frac{1}{2\pi \times f_{max}} \times \mathbf{R_{ct}} \qquad \textbf{(3.4)}$$

Where, C_{dl} = double layer capacitance

R_{ct} = charge transfer resistance

f_{max} = frequency at Z' value maximum.

Inhibition efficiency can be obtained from Nyquist plot as follows **(Tsuru *et al*, 1978)**

$$\text{Inhibition efficiency (\%)} = \frac{R_{ct(inh)} - R_{ct(blank)}}{R_{ct(inh)}} \times 100 \qquad \textbf{(3.5)}$$

where, $R_{ct(inh)}$ = charge transfer resistance in the presence of inhibitor.

$R_{ct(blank)}$ = charge transfer resistance in the absence of inhibitor.

From the measured double layer capacitance $C_{dl,}$ the surface coverage θ of inhibitor is given by **(Elakadi *et al*, 2000)**

$$\text{Surface Coverage } (\theta) = \frac{C_{dl(blank)} - C_{dl(inh)}}{C_{dl(blank)}} \qquad \textbf{(3.6)}$$

Where, $C_{dl\ (blank)}$ = the double layer capacitance in the absence of inhibitor.

$C_{dl\ (inh)}$ = the double layer capacitance in the pres ence of inhibitor.

3.2.2 Mass loss methods

The mild steel and aluminium coupons in triplicate were immersed in 100ml of inhibited and uninhibited solutions for a predetermined period of time, then removed, washed and kept in the desiccators. The specimens are weighed before immersion in the test solutions and reweighed after immersion. Weight loss experiments were done according to ASTM standard procedure **(stated in ASTM, G 1-2).** The experiments were performed for various parameters such as,

- ✶ Concentration variation from 0.1% to 0.7%
- ✶ Different time intervals: 1/2 h, 1 h, 3 h, 6 h, 12 h, 24 h.
- ✶ Various temperatures: 303 K, 313 K, 323 K, 333 K, 343K, and 353K.

From the initial and final masses of the specimen, the mass loss, corrosion rate, inhibition efficiency and surface coverage were determined using the following relationship,

Corrosion rate expressed in mills per year was calculated using the formula,

$$\text{Corrosion Rate (mpy)} = \frac{K \times W}{DAT} \qquad \textbf{(3.7)}$$

Where, K = Constant-$3.45*10^6$ (mpy), W = Mass loss in grams; D = Density of mild steel in mg / cm^3; A = Area of the specimen in cm^2; T = Exposure time in hours

$$\text{Inhibitor Efficiency (\%)} = \frac{CR_{blank} - CR_{inh}}{CR_{blank}} \times 100 \qquad \textbf{(3.8)}$$

Where, CR_{blank} = Corrosion rate of mild steel in acidic medium

CR_{inh} = Corrosion rate of mild steel in the presence of inhibitor (HR/CI)

$$\text{Surface Coverage } (\theta) = \frac{W_o - W}{W_o} \qquad \textbf{(3.9)}$$

Where, Wo = Mass loss of mild steel without inhibitor (blank).

W = Mass loss of mild steel in the presence of the inhibitor.

3.2.3Adsorption Isotherm

The phenomenon of interaction between the metal surface and inhibitors can better be understood in terms of adsorption isotherm. Adsorption provides information about the interaction among the adsorption molecules as well as their interaction with the electrode surface. The knowledge of the adsorption behaviour of the inhibitor is important to study the mechanism. For this reason, various adsorption isotherms are tested graphically to fit a suitable adsorption model for the inhibitor.

Langmuir	- Plot of log (C/θ) Vs log C	**(3.10)**
Temkin	- Plot of θ Vs log C	**(3.11)**
Freundlich	- Plot of log θ Vs log C	**(3.12)**
Frumkin	- Plot of θ Vs ln [θ / C (1- θ)]	**(3.13)**
Flory – Huggins	- Plot of log (θ/C) Vs log (1- θ)	**(3.14)**
Bockris-Swinkel's	- Plot of θ log (θ /1- θ) Vs log C	**(3.15)**
El-Awady kinetic thermodynamic	- Plot of log (θ/1- θ) Vs log C	**(3.16)**

Data were tested graphically by fitting various isotherms and statistical estimation of correlation for the curve fitting of isotherms have been used to investigate the goodness of fit of the isotherms using **SPSS 16** package

3.2.4 Kinetic parameters

Energy of Activation (E_a)

The activation energy for the corrosion of mild steel and AA1100 in 1 M HCl was calculated using the Arrhenius equation **(Radovici, 1965).**

$$CR = A \exp (-E_a/ RT) \quad \textbf{(3.17)}$$

Where CR is the corrosion rate of mild steel and AA 1100, A is Arrhenius or pre-exponential constant, E_a is the activation energy for the corrosion of mild steel, R is the gas constant and T is the temperature (**Abd-El-Rehim *et al,* 1999**). The logarithm of both sides of equation (3.17) yields equation (3.18)

$$\log CR = \log A - E_a/2.303RT \quad \textbf{(3.18)}$$

Applying the formula Ea = - 2.303 x R x Slope

Plots of log CR Versus 1/T for the corrosion of mild steel in the presence of various concentrations of HR/CI extracts yields straight lines. From slopes and intercepts of the Arrhenius plot, the values of E_a and A were computed.

The transition state equation (3.19) was used to calculate the thermodynamic parameters (enthalpy of adsorption ΔH_a and entropy of adsorption ΔS_a) for the adsorption of inhibitors on on mild steel and AA1100 surface.

$$CR/T = R/Nh \times \exp (\Delta S_a/R) \times \exp (\Delta H_a/RT) \quad \textbf{(3.19)}$$

Where CR is the corrosion rate, R is the universal gas constant (8.31434 $JK^{-1}mol^{-1}$), T is the absolute temperature, A is the pre-exponential factor, h is Planck's constant (6.626176 $\times 10^{-34}$ JS) and N is Avogadro's number (6.02252 $\times 10^{23}$ mol^{-1}).

From the logarithm of both sides of equation (3.19), equation (3.20) is obtained

$$\log (CR/T) = \log R/Nh + \Delta S_a/2.303R - \Delta H_a/2.303RT \quad \textbf{(3.20)}$$

Plots of log (CR/T) versus 1/T for the studied inhibitors were linear. The slopes and intercepts of the transition state plots, the values of ΔS_a and ΔH_a are calculated.

3.2.5 Thermodynamic Parameters

Free Energy of Adsorption ($\Delta G°_{ads}$)

The change in free energy of adsorption at high temperature at various concentrations has been calculated using the formula, (**Abd-El-Rehim *et al,* 1999**).

$$\log C = [\log (\theta/1- \theta)]-\log B \quad \textbf{(3.21)}$$

Where $\log B = -1.744 - \Delta G_{ads}/2.303\ RT$

$$- \Delta G^{o}_{ads} = 2.303\ RT\ (1.744 + \log (\theta/1- \theta) - \log C) \quad \textbf{(3.22)}$$

where, R = Gas constant (8.314 J/mole); T = Temperature in Kelvin; C = Concentration (%v/v); θ = Surface coverage.

Enthalpy ($\Delta H°_{ads}$) and Entropy ($\Delta S°_{ads}$) of Adsorption

According to Gibbs-Helmholtz relation

$$\Delta G^{\circ}_{ads} = \Delta H^{\circ}_{ads} - T\Delta S^{\circ}_{ads} \quad \textbf{(3.23)}$$

where, ΔG°_{ads} = Change in free energy of adsorption.

ΔH°_{ads} and ΔS°_{ads} = Change in enthalpy and Change in entropy.

T = Temperature.

The plot of ΔG°_{ads} Vs Temperature was drawn. The slopes of these lines are equal to ΔS°_{ads}, and the intercepts on free energy axis gives the corresponding change of enthalpy (ΔH°_{ads}) **(Eddy *et al,* 2010)**.

3.3 Phase III: Surface Analytical Techniques

- ✶ UV-Visible spectroscopy (UV)
- ✶ FT-IR Spectral Analysis
- ✶ Scanning Electron Microscope (SEM)-Energy dispersive X-ray analysis (EDX)
- ✶ X-Ray Diffraction Analysis (XRD)
- ✶ Laser Profilometer.

3.3.1 UV-Visible spectroscopy (UV)

PC based double beam spectrophotometer 2202 was used to confirm the formation of metal-inhibitor complex on mild steel/AA1100 surface.UV-visible absorption Spectrophotometric method was carried out for crude plant extract and the solution containing mild steel/AA1100 immersed in 1 M HCl with addition of 0.7% concentration of the HR /CI extracts after 3h at room temperature.

3.3.2 FT-IR Spectral Analysis

FTIR was recorded using Perkin Elmer FTIR spectrophotometer which extended from 4000 and 400 cm^{-1}.The interaction between the investigated inhibitor molecules and the metal surface has been studied by FT-IR spectra. Mild steel /AA1100 samples were immersed in inhibited 1 M HCl solution for 3 h and the results are presented for corrosion products adsorbed on the surface of MS.

3.3.3 Scanning electron microscope (SEM)- Energy dispersive X-ray analysis (EDX)

SEM was used to study the topography of the mild steel/AA1100 in the presence and absence of the inhibitors. Mild steel/AA1100 specimens immersed in 1 M HCl in the absence and presence of HR/CI extracts for 3h were examined by SEM using a **JEOL MODEL JSM 6390** .The elemental composition of the mild steel/AA1100 specimens after exposure to 1 M HCl in the absence and presence of HR/CI extracts was analyzed by EDX.

3.3.4 X-Ray Diffraction Analysis

XRD patterns of the film formed on the metal surface were recorded using a computer-controlled, XPERT-PRO **X-ray diffractometer.** The mild steel/AA1100 specimens after exposure to 1 M HCl solution in the absence and presence of HR/CI extracts for 3h were examined by XRD.

3.3.5 Laser Profilometer

Surface profiles and pores were studied using a Zeta-20 3D Optical Profiler. Mild steel/AA1100 specimens kept in a vacuum desiccator after the inhibition test were mounted on sample holder occurred under the objective of the Optical Profiler and the 3D photos were taken from the 100x magnified surface via operating program on computer. The mild steel specimens after exposure to 1 M HCl solution in the absence and presence of HRL/HRF/CIL/CIF extracts for 3h were examined by Zeta 2D and3D Profiler.

3.4 Phase IV: Quantum chemical studies using Mopac software.

Quantum-chemical calculations were useful approach to investigate the mechanism of reaction in the molecule and its electronic structure levels. The structure and electronic parameters can be obtained by means of theoretical calculations **(Ebenso and Ekpe, 1996).**Quantum chemical calculations were performed using Mopac software.Certain electronic structure parameters have been correlated with the effectiveness of adsorption type inhibitors. These include the frontier molecular orbitals, namely, the highest occupied molecular orbital (HOMO) and lowest unoccupied molecular orbital (LUMO) which are evaluated for selected phytochemical constituents present in the studied extracts using the following equations:

Ionisation potential (IP) and electron affinity (EA) were calculated from E_{HOMO} and E_{LUMO}

$$\text{Ionisation potential (IP)} = - E_{HOMO} \quad \textbf{(3.24)}$$

$$\text{Electron Affinity (EA)} = - E_{LUMO} \quad \textbf{(3.25)}$$

The ground state energy E(ρ) of an atom/molecule can be expressed in terms of its electron density. Using the finite difference approximation, the global softness σ can be evaluated. The global hardness η, which is the inverse of the global softness can be evaluated using the following equations: **(Martinez, 2002; Chattaraj *et al,* 2007)**.

$$\text{Energy gap } (\Delta E) = E_{HOMO} - E_{LUMO} \quad \textbf{(3.26)}$$

$$\text{Global Hardness } (\eta) = \frac{E_{HOMO} - E_{LUMO}}{2} \quad \textbf{(3.27)}$$

$$\text{Global Softness } (\sigma) = \frac{1}{2\eta} \quad \textbf{(3.28)}$$

$$\text{Electronegativity } (\chi) = \frac{IP + EA}{2} \quad \textbf{(3.29)}$$

$$\text{Electrophilic Index } (\omega) = \frac{\mu^2}{2\eta} \quad \textbf{(3.30)}$$

where, E_{HOMO} = Highest occupied molecular orbital.

E_{LUMO} = Lowest unoccupied molecular orbital.

μ= Dipole moment.

If bulk iron metal and the inhibitor molecule are brought together, the flow of electrons will occur from the molecule of lower electronegativity to the iron that has higher electronegativity until the value of the chemical potential becomes equal. The fraction of electrons transferred from the inhibitor molecule to the iron atom will then be given by

$$\Delta N_{Fe} = (\chi_{Fe} - \chi_{inh}) / 2(\eta_{Fe} + \eta_{inh}) \quad \textbf{(3.31)}$$

$$\Delta N_{Al} = (\chi_{Al} - \chi_{inh}) / 2(\eta_{Al} + \eta_{inh}) \quad \textbf{(3.32)}$$

where χ_{Fe}, χ_{Al},χi_{nh} represent the absolute electronegativity of iron,aluminium and the inhibitor molecule, respectively and $\eta_{Fe} + \eta_{inh,}$ $\eta_{Al} + \eta_{inh,}$ represent the absolute hardness of iron and the inhibitor molecule.

The aim of this investigation is to compute the relevant electronic properties by means of semiempirical parameterisation to generate accurate information that enables better understanding of the inhibitory behaviour exhibited by HR/CI components.

3.5 Softwares used for the present investigation

The softwares used for the present is given in Figure 3.2

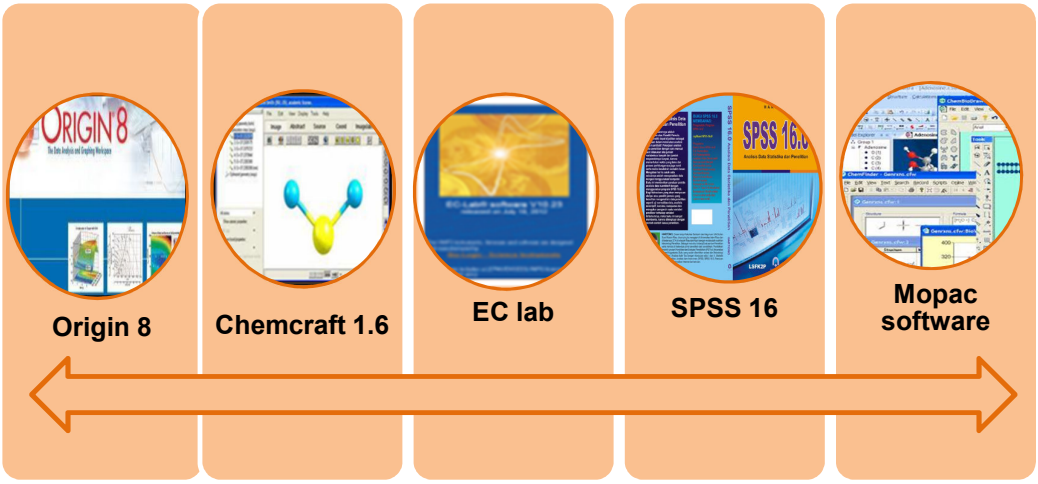

Figure 3.2- software Tools used

3.6 Experimental frame work

Work plan carried out in the current investigation is depicted in the flow chart (Figure 3.3).

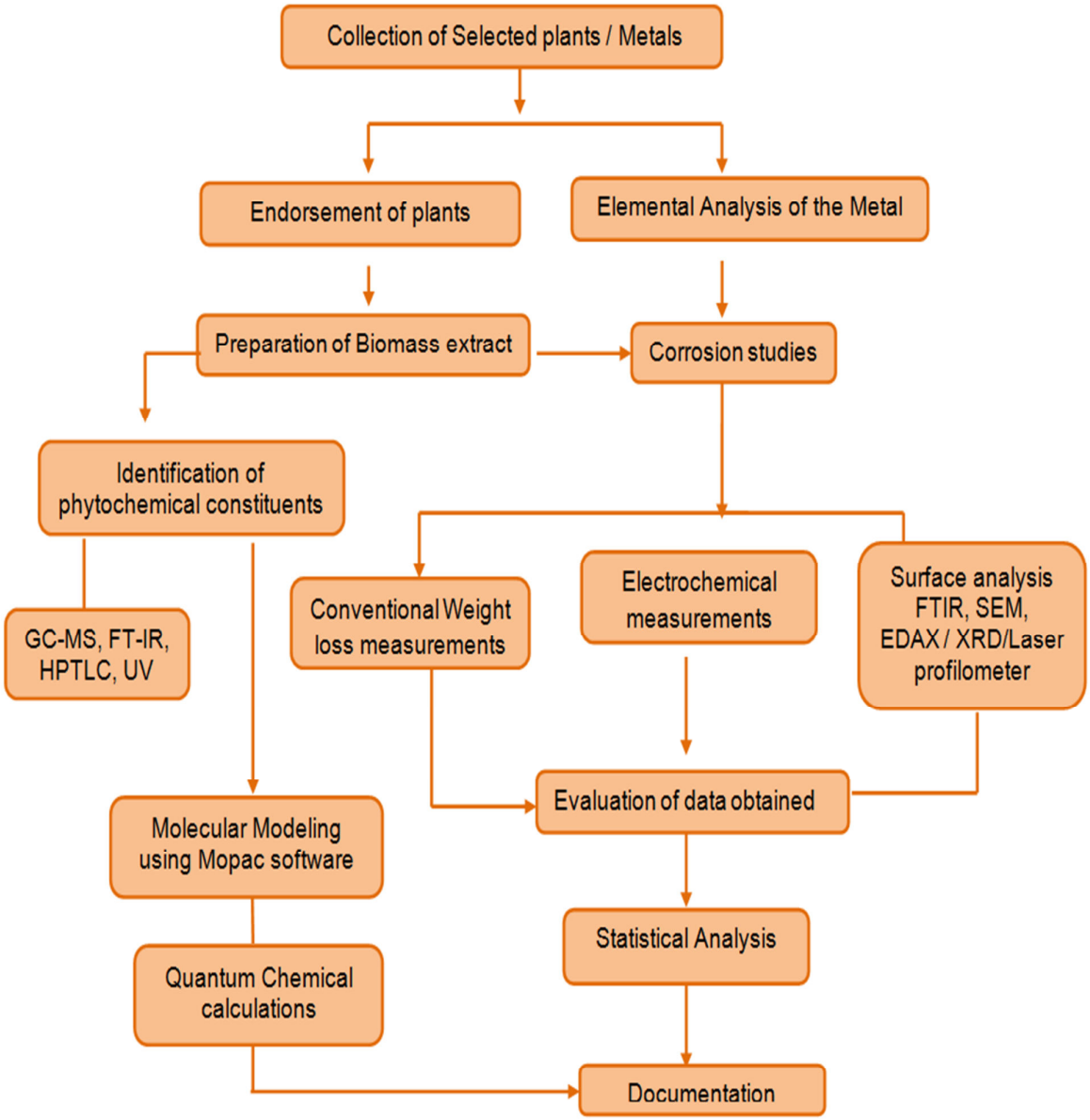

Figure 3.3 Proposed framework of Methodology

The methodology described in this chapter was adopted for the present investigation and the findings are presented and discussed in chapter IV.

4

Results and Discussion

The results of the present work entitled "**Corrosion Inhibition and Adsorption Potential of Biomass Extracts-Leaves and Flowers of *Heliconia rostrata and Canna indica* on Corrosion of Mild Steel/Aluminium 1100 in 1 M HCl"** are discussed under the following headings in the light of the objectives set forth.

Phase I : Characterization of selected Biomass extracts

Phase II : Methods adopted-Electrochemical & Mass loss measurements

Phase III : Surface Analytical Techniques

Phase IV : Theoretical calculation using Mopac software.

Phase I:

4.1 Characterization of selected Biomass extracts

The following techniques were carried out to characterise the selected biomass extracts-*Heliconia rostrata* leaves (HRL), *Heliconia rostrata* flowers (HRF), *Canna indica* leaves (CIL) and *Canna indica* flowers (CIF)

4.1.1 Phytochemical screening

4.1.2 HPTLC

4.1.3 GC-MS

4.1.4 FT-IR

4.1.5 UV

Phase II:

Methods adopted - Electrochemical & Mass loss measurements

4.2 Electrochemical measurements

4.2.1 Potentiodynamic polarisation studies of Mild steel in 1 M HCl with and without HRL, HRF, CIF, CIL extracts.

4.2.2 Electrochemical impedance measurements of Mild steel in 1 M HCl with and without HRL, HRF, CIF, CIL extracts.

4.2.3 Potentiodynamic polarisation studies of AA1100 in 1 M HCl with and without HRL, HRF, CIF, CIL extracts

4.2.4 Electrochemical impedance measurements of AA1100 in 1 M HCl with and without HRL, HRF, CIF, CIL extracts.

4.3 Mass loss Measurements

4.3.1 Effect of concentration of HRL, HRF, CIL, CIF extracts and period of immersion on corrosion of mild steel in 1 M HCl.

4.3.2 Influence of temperature on the corrosion of mild steel in the presence of HRL, HRF, CIL and CIF extracts.

4.3.3 Effect of concentration of HRL, HRF, CIL,CIF extracts and period of immersion on corrosion of AA1100 in 1 M HCl.

4.3.4 Influence of temperature on the corrosion of AA1100 in the presence of HRL, HRF, CIL and CIF extracts.

4.3.5 **Adsorption isotherm**

Statistical Analysis was carried out to investigate whether the inhibitor system is statistically significant or not by doing F- tests by using the Analysis of Variance ANOVA

4.3.6 **Activation Parameters for inhibition process**

Activation energy, Enthalpy and Entropy of activation

4.3.7 **Thermodynamic adsorption parameters**

Free energy, Enthalpy and Entropy of adsorption

Phase III :

4.4 Surface Analytical Techniques

The following surface analytical techniques were used to study the surface of mild steel and aluminium in the absence and presence of selected biomass extracts.

4.4.1 UV Visible spectral Analysis

4.4.2 FT-IR Spectral studies

4.4.3 X-ray diffraction Analysis

4.4.3 Scanning Electron Microscopic studies

4.4.4 Energy dispersive X-ray analysis

4.4.5 Study of roughness by 3D optical profilometry

Phase IV:

4.5 Theoretical calculation using Mopac software

Quantum chemical calculations are carried out to interpret the experimental results with theoretical calculations.

4.1 Characterization of *Heliconia rostrata* (HR) and *Canna indica* (CI) extracts

4.1.1 Phytochemical screening of selected biomass extracts

The preliminary phytochemical screening tests may be useful in the detection and identification of chemical constituents present in the biomass extracts. Further, the presence of different phytoconstituents in the extracts may be responsible for corrosion inhibition. Phytochemical screening tests were carried out in the selected biomass extracts using the standard procedures as described by **Harborne, 1973**. The investigated plant extracts were screened for the presence of flavonoids, alkaloids, terpenoids, saponins, tannins, reducing sugar, polyphenols and anthraquinones.

Table : 4.1 Preliminary phytochemical screening of the crude extracts of HR/CI

Phytochemical constituents	HR		CI	
	Leaves	Flowers	Leaves	Flowers
Alkaloids	-	-	+	++
Carbohydrates	+	++	+	+
Flavonoids	+	++	+	++
Glycosides	-	-	+	+
Phlobatinins	-	-	+	+
Proteins	+	++	+	+
Anthroquinone	-	-	-	-
Saponins	-	+	+	++
Steroids	-	-	+	++
Terpenoids	+	++	+	++
Tannin	+	-	+	+
Coumarine	+	+	-	-
Phenolic compounds	+	+	+	+

(+) = indicate presence ++ =moderate amount (-) = indicate absence

The results indicated the presence of terpenoids, coumarin and phenolic compounds in HRL and HRF extracts. Similarly for CIL and CIF extracts presence of alkaloids, flavonoids, saponins, steroids and terpenoids are detected. These results reflect the presence of a broard spectrum of secondary metabolites containing 'N' and 'O' rich centres in them.

4.1.2 HPTLC

HPTLC is an analytical tool to identify the presence of terpenoid, flavonoid and coumarin present in the plant extracts. A detailed report of the phytochemical constituents

present in *Canna indica* has already been reported in the literature (**Bachhet *et al*, 2013**) and in the present study HPTLC analysis is carried for ethanol extracts of leaves and flowers of ***Heliconia rostrata*** (HRL, HRF) only.

4.1.2.1 HPTLC analysis of ethanol extracts of HRL and HRF

To find out the presence of terpenoid, flavonoid and coumarin present in the ethanol extract of HRLE and HRFE, different compositions of the mobile phase of HPTLC analysis are tested to obtain high resolutions and reproducible peaks. The desired solvent system for terpenoid has been achieved using n-Hexane-Ethyl acetate (7.2:2.9), for the flavonoid it is Ethyl acetate-Butanone-Formic acid-Water (5:3:1:1) and for Coumarins it is found to be toluene-Diethylether (1:1) saturated with 10% Glacial acetic acid.

a) Terpenoid profile of *ethanol extracts of* HRL and HRF

The ethanolic extract of the plant HRL and HRF reflects the presence of nineteen different type of terpenoids with Rf values *0.*07,0.12,0.23,0.25,0.30,0.43,0.47,0.61,0.64, 0.72,0.76,0.82,0.89,*0.97,*0.822,0.74,0.07,0.12,0.86,0.94 and 0.97 (Table 4.2). Blue, Violet coloured zone observed from the chromatogram after derivatization, confirms the **presence of Terpenoid.**

Table: 4.2 Terpenoid profile of HRL and HRF

Track	Peak	Rf	Height	Area	Assigned substance
Sample HRL	1	0.07	11.4	110.7	Unknown
Sample HRL	2	0.12	19.1	366.6	Unknown
Sample HRL	3	0.23	10.4	198.6	Unknown
Sample HRL	4	0.25	15.2	243.0	Unknown
Sample HRL	5	0.30	15.6	289.7	Unknown
Sample HRL	6	0.43	24.1	545.1	Unknown
Sample HRL	7	0.47	38.2	903.7	Unknown
Sample HRL	8	0.61	26.6	393.7	Terpenoid 1
Sample HRL	9	0.64	40.7	1193.7	Terpenoid 2
Sample HRL	10	0.72	83.2	2634.4	Terpenoid 3
Sample HRL	11	0.76	156.1	5843.2	Terpenoid 4
Sample HRL	12	0.82	185.0	6499.4	Terpenoid 5
Sample HRL	13	0.89	162.2	6434.8	Terpenoid 6
Sample HRL	14	0.97	339.2	9065.0	Terpenoid 7
STD	1	0.87	390.8	14648.5	Terpenoid standard
Sample HRF	1	0.22	10.7	292.9	Unknown
Sample HRF	2	0.74	142.8	5604.6	Terpenoid 1
Sample HRF	3	0.86	103.9	4609.0	Terpenoid 2
Sample HRF	4	0.94	58.5	1449.9	Terpenoid 3
Sample HRF	5	0.97	145.7	2730.7	Terpenoid 4

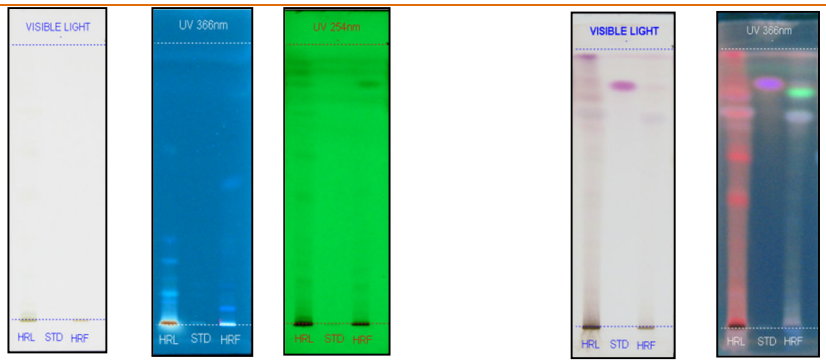

Before derivatization **After derivatization**

Figure 4.1: Terpenoid chromatogram of ethanol extracts of HRL and HRF before and after derivatization.

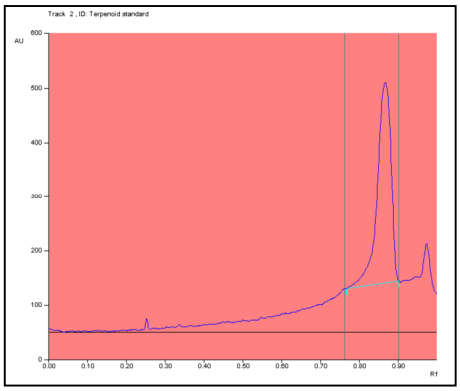

Terpenoid standard- Baseline display (Scanned at 500 nm)

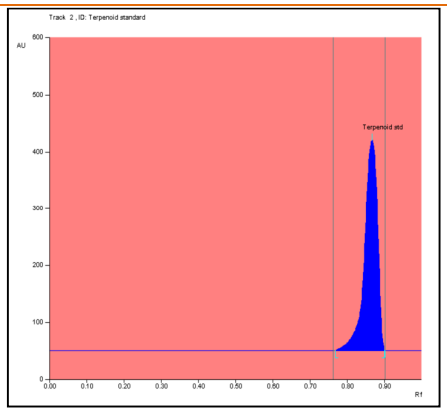

Terpenoid standard- Peak densitogram display (Scanned at 500 nm)

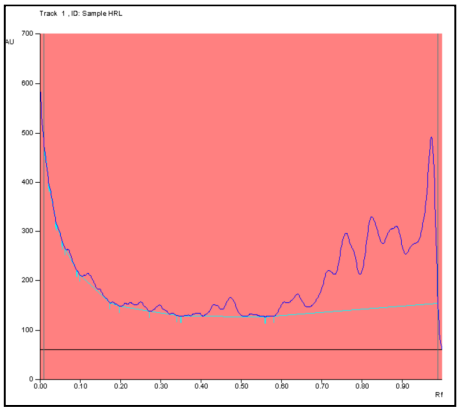

HRL extract - Baseline display (Scanned at 500 nm)

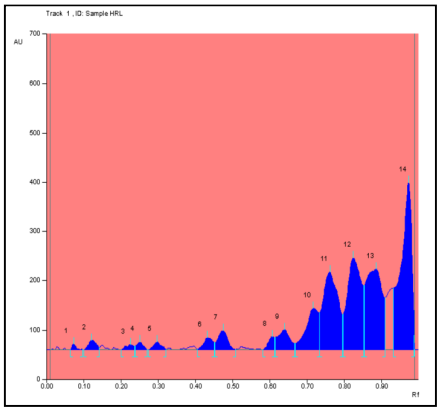

HRL extract - Peak densitogram display (Scanned at 500 nm)

Figure 4.2 : Baseline and peak densitogram display of HRL extract with standard for Terpenoid profile.

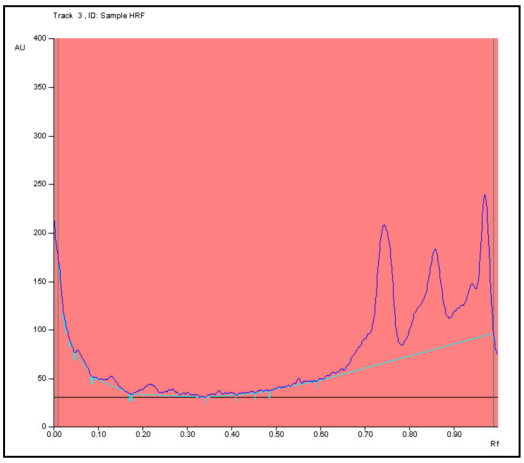

HRF extract-Baseline display
(Scanned at 500 nm)

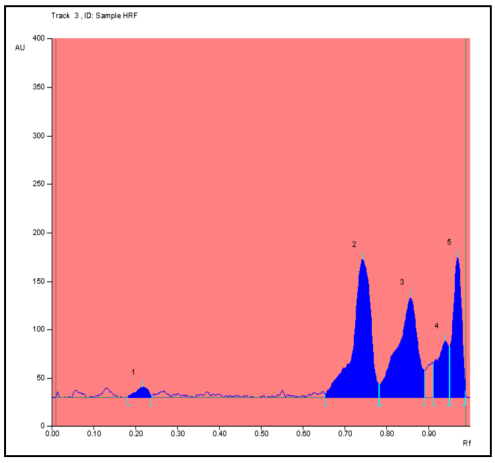

HRF extract-Peak densitogram display
(Scanned at 500 nm)

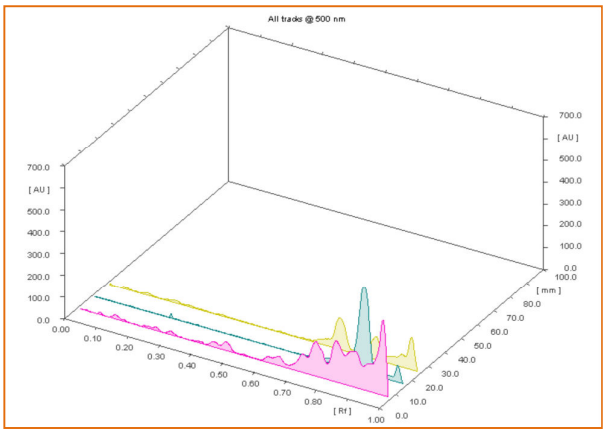

3D display of all Tracks

Figure 4.3 : Baseline and peak densitogram display of HRF extract and 3D display of all Tracks for terpenoid profile.

b) Flavonoid profile of HRL and HRF extracts

The ethanolic extract of HRL,HRF showed the presence of eleven different type of flavonoid with Rf values 0.17,0.22,0.30,0.49,0.57,0.65,0.81,0.97,0.07,0.35 and 0.96 (Table 4.3). Yellow, Yellowish blue coloured fluorescent zone after derivatization confirms the **presence of Flavonoid.**

Table : 4.3 Flavonoid profile of HRL and HRF extracts

Track	Peak	Rf	Height	Area	Assigned substance
Sample HRL	1	0.17	17.0	318.8	Unknown
Sample HRL	2	0.22	97.8	2375.3	Flavonoid 1
Sample HRL	3	0.30	14.5	420.9	Unknown
Sample HRL	4	0.49	48.9	2364.6	Flavonoid 2
Sample HRL	5	0.57	238.0	9191.3	Flavonoid 3
Sample HRL	6	0.65	147.1	5104.0	Flavonoid 4
Sample HRL	7	0.81	23.3	525.6	Flavonoid 5
Sample HRL	8	0.97	187.5	4743.6	Unknown
STD	1	0.49	590.3	22669.0	Flavonoid Standard
Sample HRF	1	0.07	13.9	188.6	Unknown
Sample HRF	2	0.35	19.5	600.6	Flavonoid 1
Sample HRF	3	0.96	126.9	3561.3	Flavonoid 2

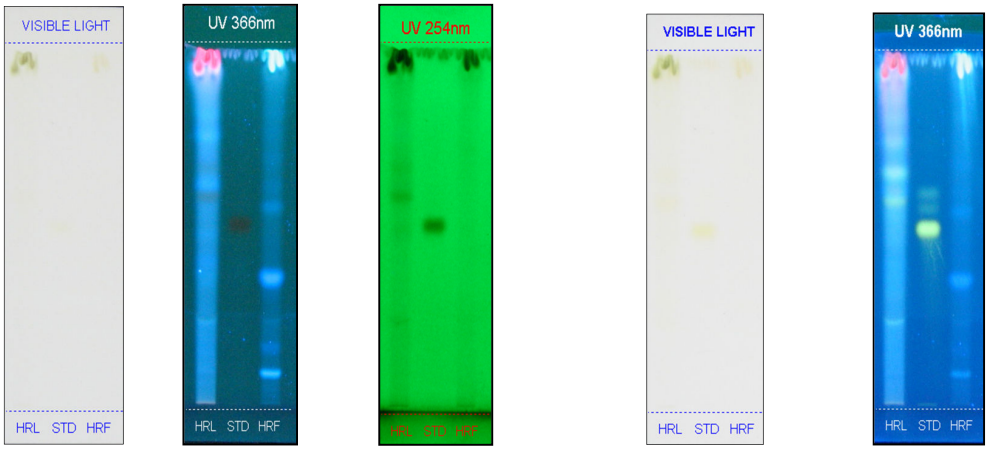

Before derivatization **After derivatization**

Figure 4.4: Flavonoid chromatogram of ethanol extracts of HRL and HRF before and after derivatization

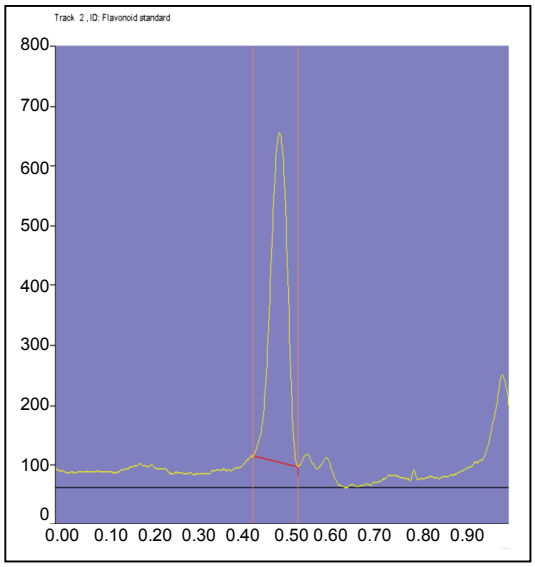

Flavonoid standard Baseline display (Scanned at 366 nm)

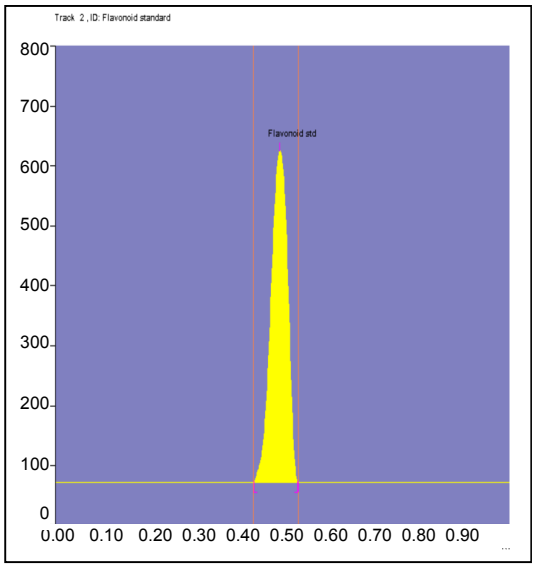

Flavonoid standard Peak densitogram display (Scanned at 366 nm)

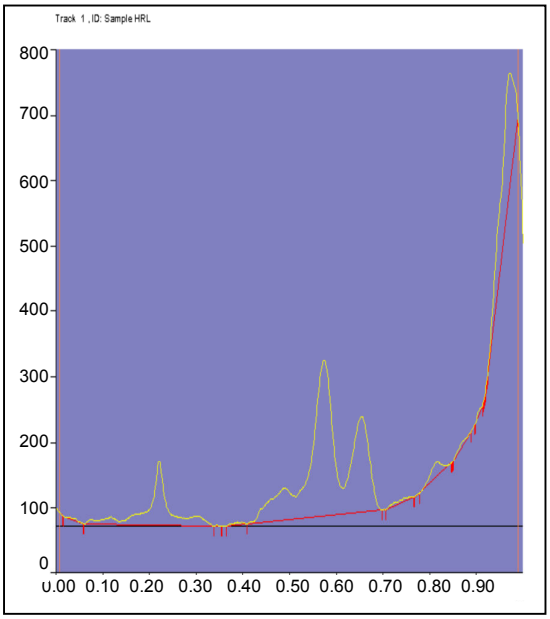

HRL extract - Baseline display (Scanned at 366 nm)

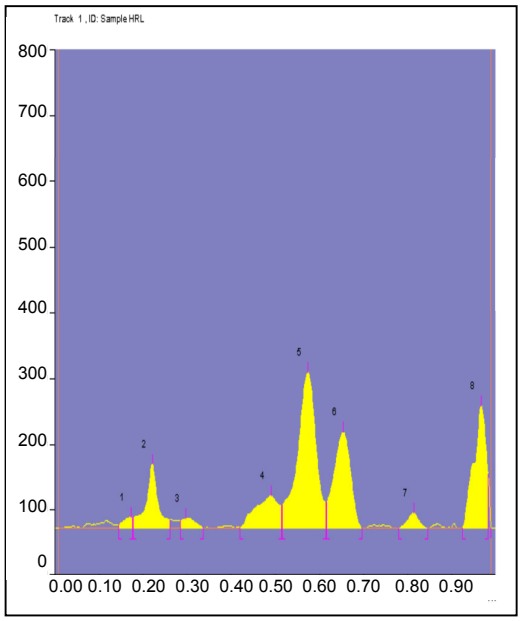

HRL extract - Peak densitogram display (Scanned at 366 nm)

Figure 4.5: Baseline and peak densitogram display of HRL extract with standard for Flavonoid profile.

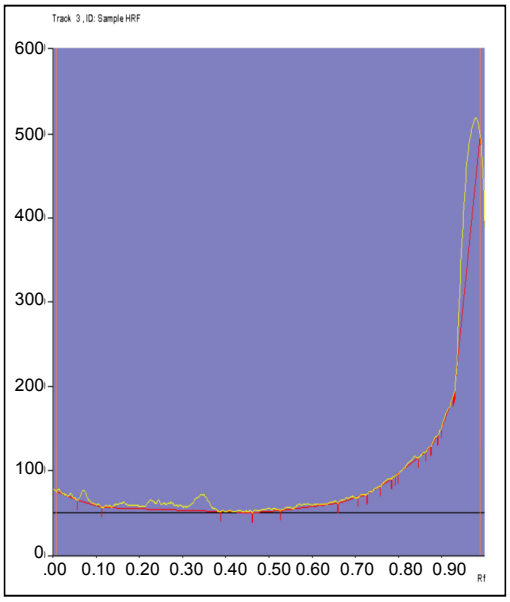

HRF extract -Baseline display
(Scanned at 366 nm)

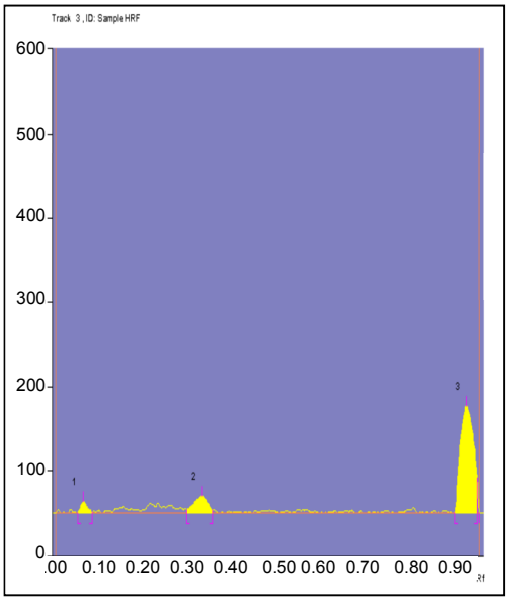

HRF extract - Peak densitogram
display(Scanned at 366 nm)

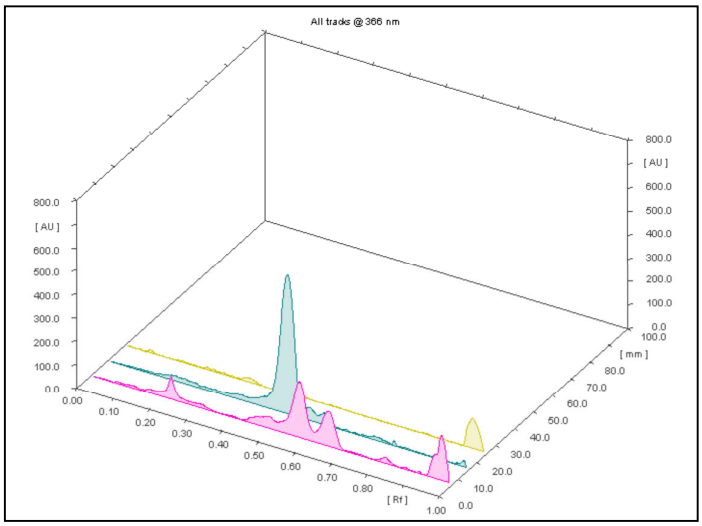

3D display of all Tracks

Figure 4.6: Baseline and peak densitogram display of HRF extract, 3D display of all Tracks for Flavonoid profile.

c) Coumarin profile of ethanol extract of HRL and HRF

The ethanolic extract of HRL,HRF indicates the presence of twenty six different type of coumarins with Rf values 0.01,0.03,0.060.15,0.23,0.26,0.42,0.48,0.60,0.66,0.77,0.86,0.91,0.94,0.98,0.06,0.14,0.21,0.25,0.36,0.53,0.57,0.60,0.71,0.83 and 0.96 (Table 4.4). Blue, Yellowish blue coloured fluorescent zone at UV 366nm after derivatization confirms the **presence of Coumarin.**

Table: 4.4 Coumarin profile of HRL and HRF extract

Track	Peak	Rf	Height	Area	Assigned substance
Sample HRL	1	0.01	43.7	194.1	Unknown
Sample HRL	2	0.03	60.8	406.0	Unknown
Sample HRL	3	0.06	26.8	293.8	Unknown
Sample HRL	4	0.15	11.1	188.0	Unknown
Sample HRL	5	0.23	55.3	1333.4	Unknown
Sample HRL	6	0.26	43.3	900.6	Unknown
Sample HRL	7	0.42	12.0	252.6	Unknown
Sample HRL	8	0.48	85.2	2035.5	Unknown
Sample HRL	9	0.60	19.9	521.7	Unknown
Sample HRL	10	0.66	85.8	4202.6	Unknown
Sample HRL	11	0.77	61.6	2285.1	Unknown
Sample HRL	12	0.86	14.5	409.8	Unknown
Sample HRL	13	0.91	26.4	800.2	Unknown
Sample HRL	14	0.94	14.4	261.5	Unknown
Sample HRL	15	0.98	15.5	141.9	Unknown
STD	1	0.70	88.3	5227.2	Coumarin standard
Sample HRF	1	0.06	39.0	535.3	Unknown
Sample HRF	2	0.14	20.3	369.5	Unknown
Sample HRF	3	0.21	39.0	955.4	Unknown
Sample HRF	4	0.25	47.5	1098.6	Unknown
Sample HRF	5	0.36	18.2	525.8	Unknown
Sample HRF	6	0.53	16.8	292.0	Unknown
Sample HRF	7	0.57	65.9	2016.9	Coumarin 1
Sample HRF	8	0.60	41.7	1749.3	Unknown
Sample HRF	9	0.71	41.4	1814.9	Coumarin 2
Sample HRF	10	0.83	36.0	1509.9	Coumarin 3
Sample HRF	11	0.96	14.8	212.0	Unknown

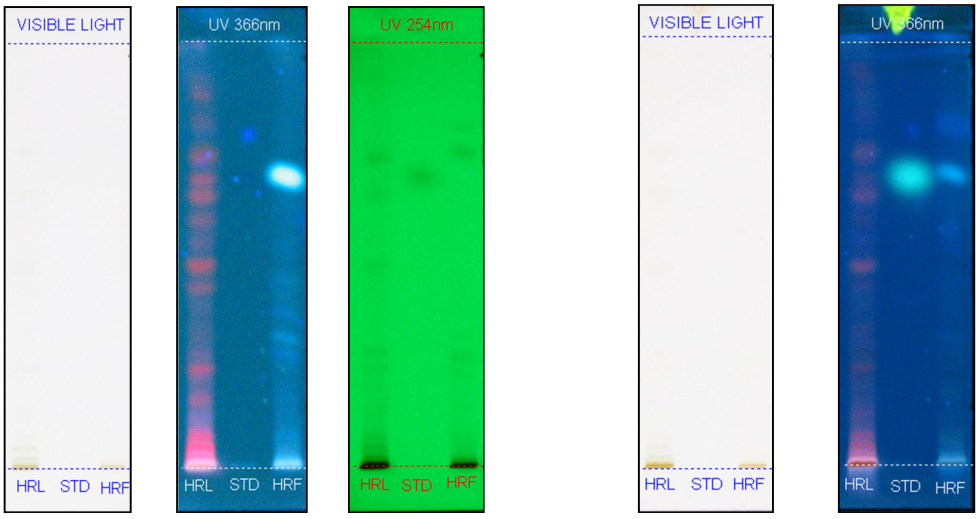

Figure 4.7. Coumarin chromatogram of ethanol extracts of HRL and HRF before and after derivatization.

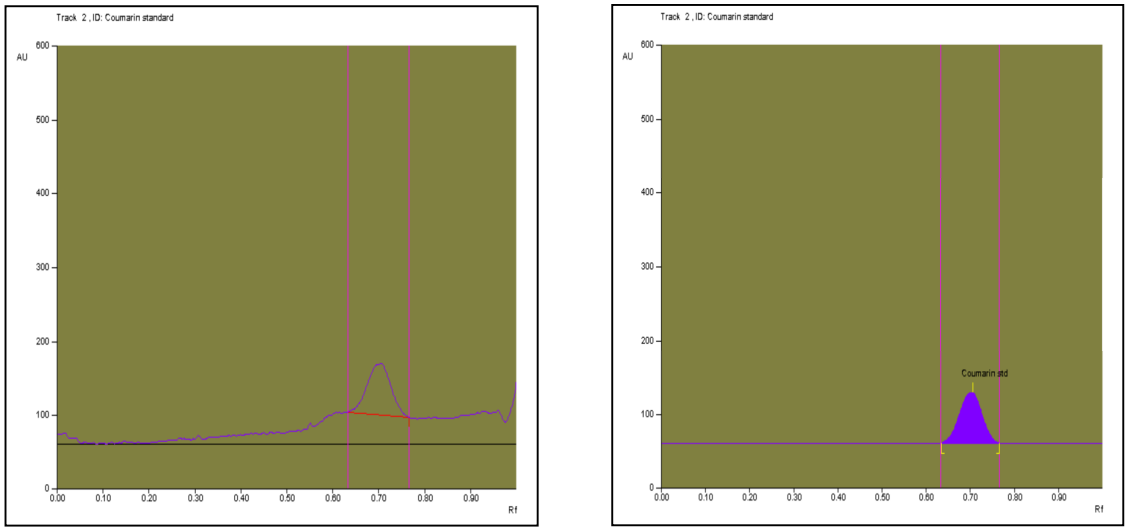

Coumarin standard -Baseline display (Scanned at 366 nm)

Coumarin standard-Peak densitogram display (Scanned at 366 nm)

Figure 4.8: Coumarin standard **-**Baseline and peak densitogram display

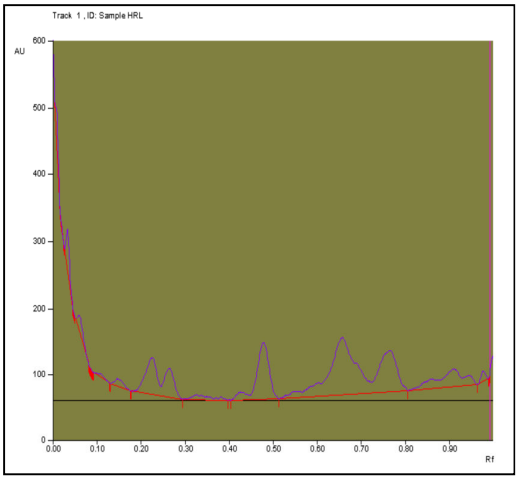

HRL extract - Baseline display
(Scanned at 366 nm)

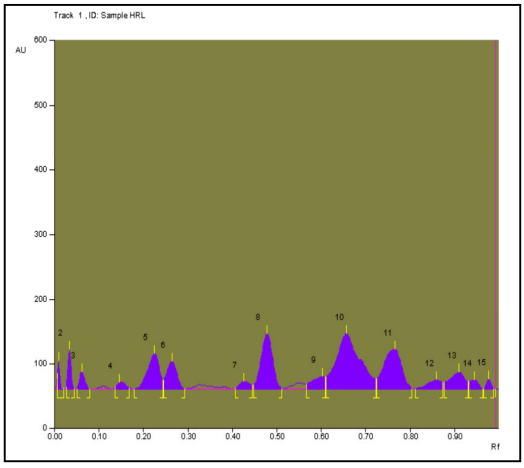

HRL extract - Peak densitogram display
(Scanned at 366 nm)

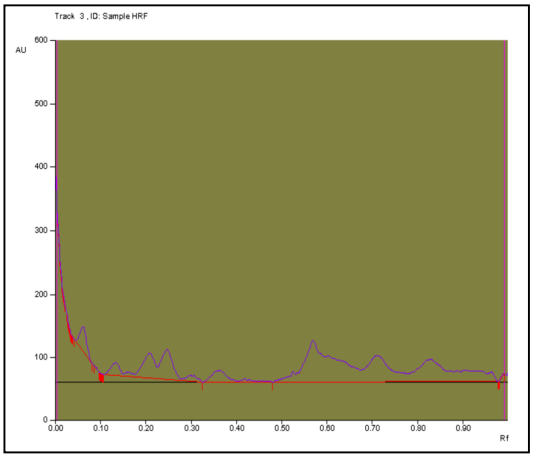

HRF extract - Baseline display
(Scanned at 366 nm)

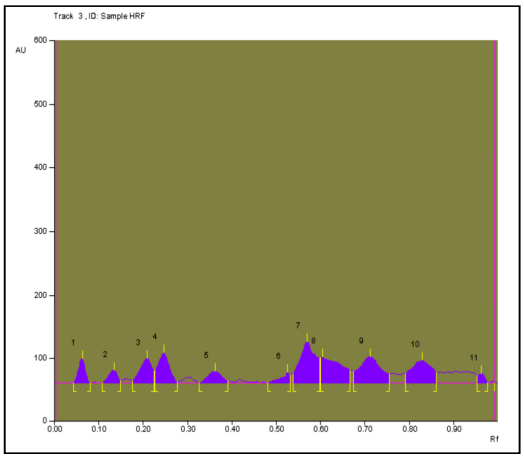

HRF extract -Peak densitogram display
(Scanned at 366 nm)

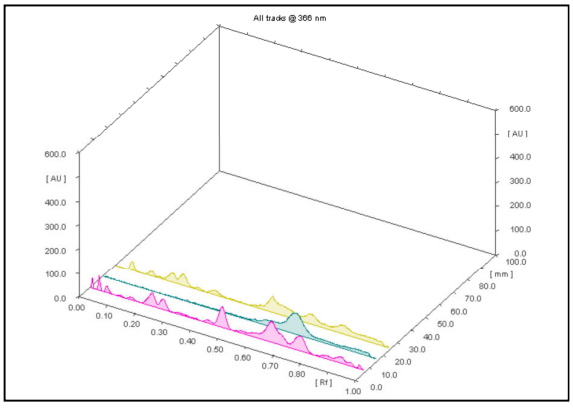

Figure 4.9: Baseline and peak densitogram display of HRL, HRF extracts and 3D display of all Tracks for coumarine pro

The HPTLC analysis of ethanol extracts of HRL, HRF reveals the presence of terpeniods, coumarines and Flavonoids. These results are supported by the phytochemical screening test.

4.1.3 GC-MS Analysis

4.1.3.1 GC-MS analysis of HRL extract

The GC spectrum of HRL extract shown in Figure 4.10 exhibits peaks at retention time 14.14, 14.55, 14.88, 15.22, 15.62 and 15.71. The mass spectra of GC peaks at retention times 14.14 and 14.55 are presented in Figure 4.10.

The mass spectrum of GC peak of HRL extract at retention time 14.14 shows molecular ion peak at m/z 429 and base peak at m/z 229. The spectrum shows various characteristic peaks at m/z 359, 299, 151 corresponds to M^+ -42, M^+ -46, indicating the presence of oxygen functionality. Also M^+ - 18 peak is noticed at m/z 211 and M^+ -61 peaks are noted at m/z 75 confirming the presence of –OH and -CH_2COOH moieties present in the extract constituents. Hence the phytochemical compound may contain hydroxyl and acid functional groups. Similar trend is also seen for the mass fragmentation patterns of other compounds present in HRL extract at retention time 14.55, 14.88, 15.22, 15.62 and 15.71. **The mass fragmentation pattern present in the extract indicates that the extract may contain the phytochemical compounds with hydroxyl and acid groups.**

4.1.3.2 GC-MS Analysis of HRF extract

The GC spectrum of HRF extract (Figure 4.11) exhibits peaks at retention time 14.33, 14.70, 15.42, 15.75 along with the MS pattern of the GC peaks noted at 14.33 and 15.42. The mass spectrum of GC peak of 14.33 retention time reflects molecular ion peak at m/z 429 and base peak at m/z 229. The spectrum shows a characteristic M^+- 49 peak at m/z 429, indicating the loss of –HO_3 group. M^+- 48 and M^+- 46 peaks are found at m/z 151 and m/z 105 which relates the presence of oxygen functionality. M^+- 30 peak observed at m/z 269, may be due to the loss of CH_2O. Hence the compound may contain oxygen containing functional groups. Similar trend is also observed for the mass fragmentation patterns for the other compounds present in HRF extract at retention time 14.70, 15.42 and 15.75. **Hence the extract may contain oxygen containing groups.**

4.1.3.3 GC-MS Analysis of CIL extract

The GC spectrum of CIL extract exhibits 12 peaks at retention time 3.80, 11.28, 16.92, 23.61, 25.43, 33.08, 33.89, 36.11, 36.77 & 37.88 (Figure 4.12). The mass spectrum

of GC- peak of CIL extract at retention time 11.28, displays molecular ion peak at m/z 359 and base peak at m/z 63. The characteristic M^+- 60 peak at m/z 299 reveals loss of $–CH_2COOH$ group. Hence the compound may contain carboxylic functional group. Also M^+- 75 peak at m/z 94 of retention time 16.92 is observed due to the loss of $-COOC_2H_5$ indicating that the extract contains ester. The mass spectrum of GC- peak of CIL extract at retention time 36.11 shows M-30 and M-40 peaks evidencing the presence of nitrogen containing compounds. The M- 18 peak which was seen at m/z 73 is due of presence of –OH group. **Hence the compound may contain nitrogen and hydroxyl groups respectively.**

Similar spectrum is noticed for the MS of other compounds present in CIL extract at retention times 3.80, 16.92, 23.61, 25.43, 33.08, 33.89, 36.77 and 37.88. **This confirms the presence of nitrogen containing compounds probably alkaloids, esters and acids in CIL extract.**

4.1.3.4 GC-MS Analysis of CIF extract

The GC-MS spectrum of CIF extract (presented in Figure 4.13) exhibits peaks at retention time 12.32, 14.24, 15.02, 15.62, 15.71 and 16.62. The mass spectrum of GC-peak of CIF extract at retention time 12.32 shows molecular ion peak at m/z 419 and base peak at m/z 229. The M^+- 60 peak at m/z 299 indicates the loss of $–CH_2COOH$ group. Hence the compound may contain an acidic functional group. The M-30 peak observed at m/z 269 of retention time 14.24 indicates the presence of $–CH_2NH_2$ group. Hence the compound may be a nitrogen containing compound. The M^+- 19 peak observed at m/z 299 of retention time 15.71, may be due to the loss of H_3O^+, confirming the **presence hydroxyl groups.**

Similar M^+- 60, M-30, M^+- 19 peaks are present in the fragmentation patterns for the of other compounds present in CIF extract at retention times 15.02, 15.62, 15.71 and 16.62. **This confirms the presence of nitrogen containing compounds probably alkaloids and acids in CIF extract.**

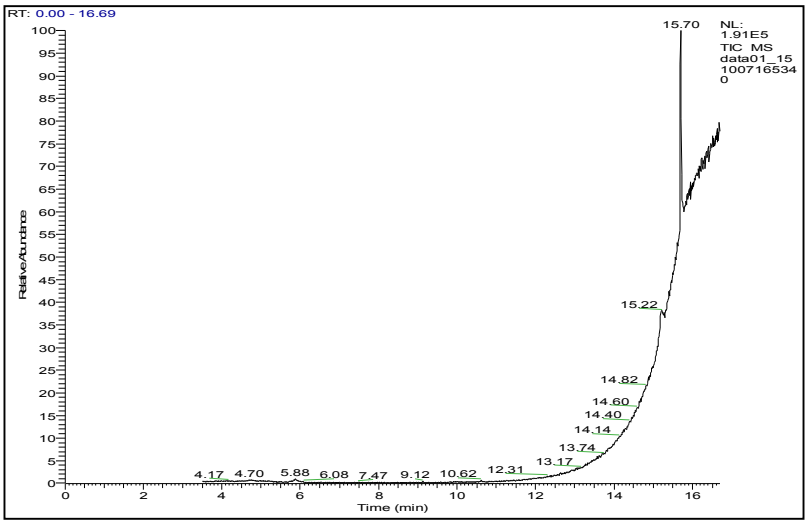

GC-MS

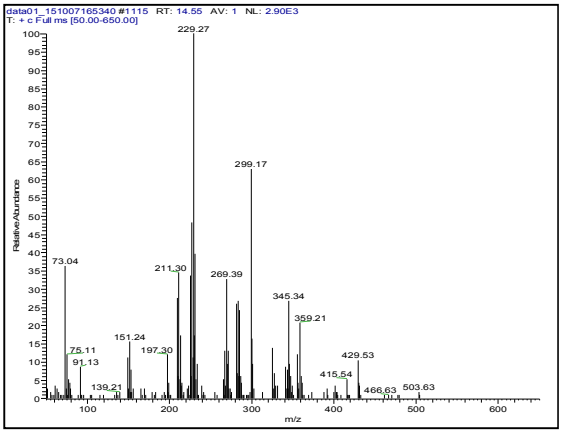

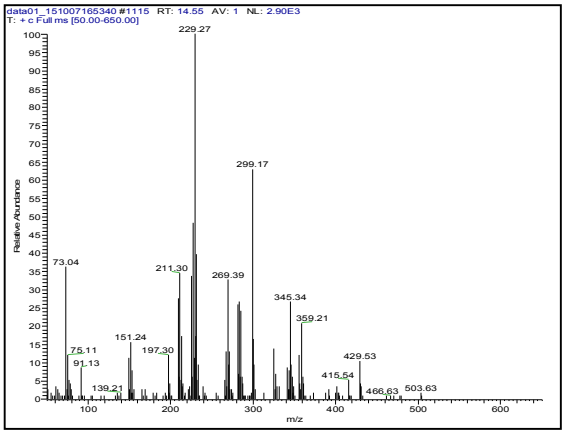

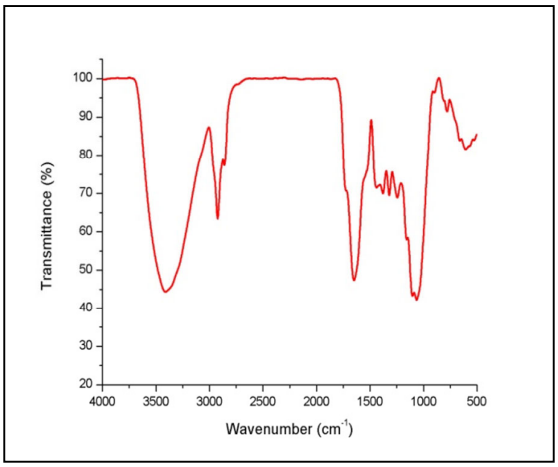

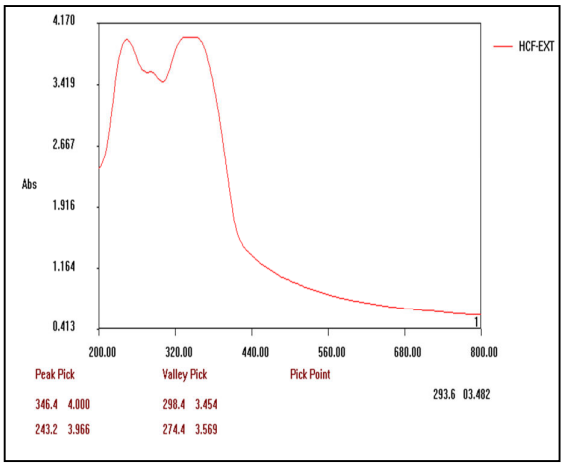

FTIR **UV**

Figure 4.10 : Characterization of HRL extract

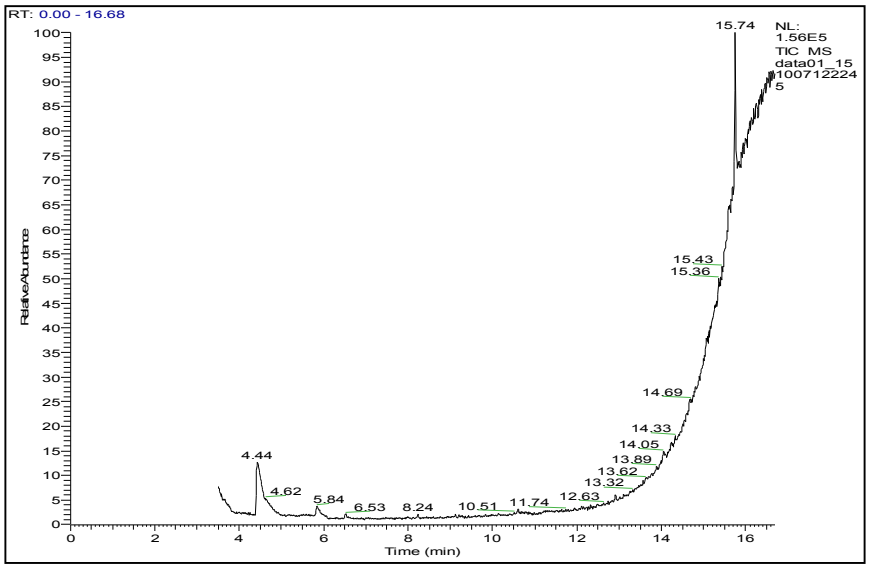

GC-MS

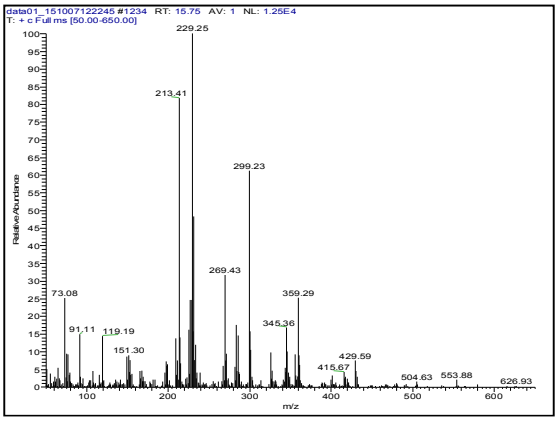

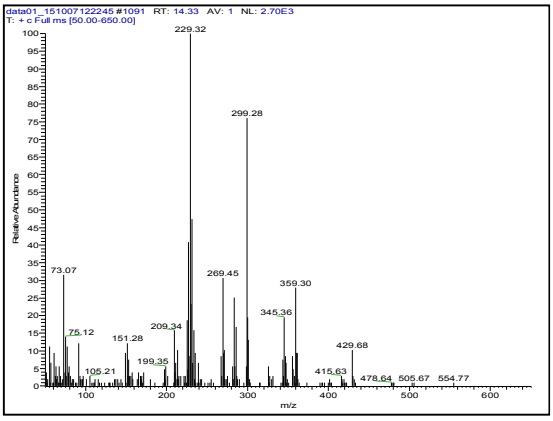

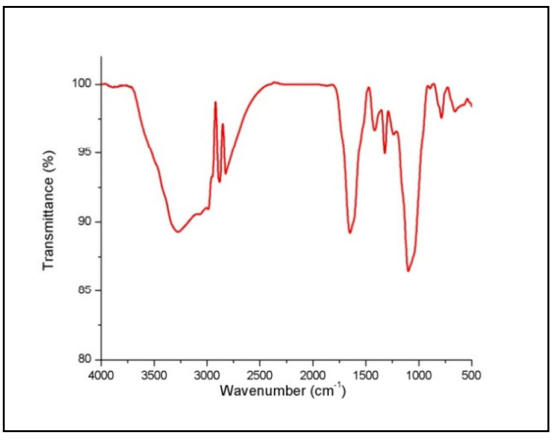

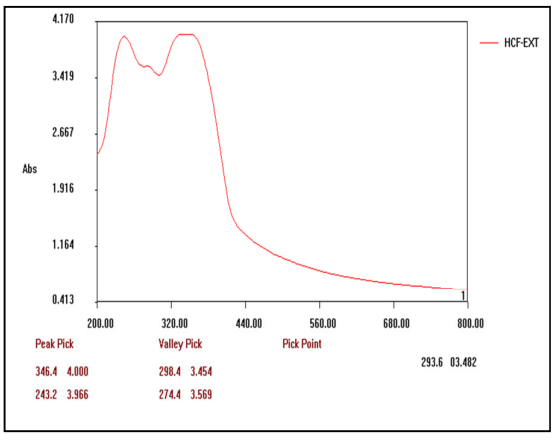

FTIR **UV**

Figure 4.11: Characterization of HRF extract

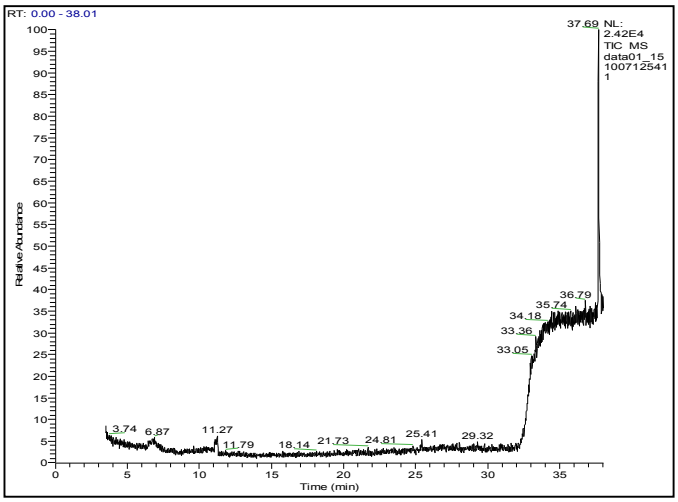

GC-MS

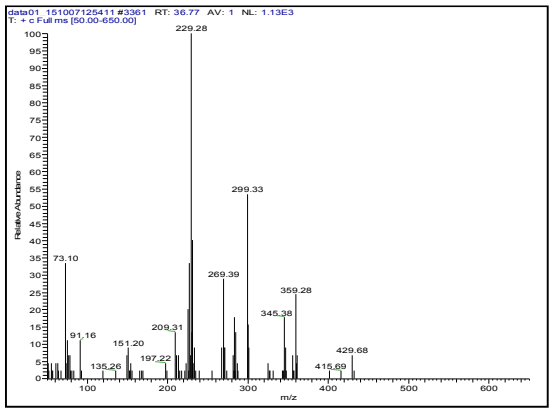

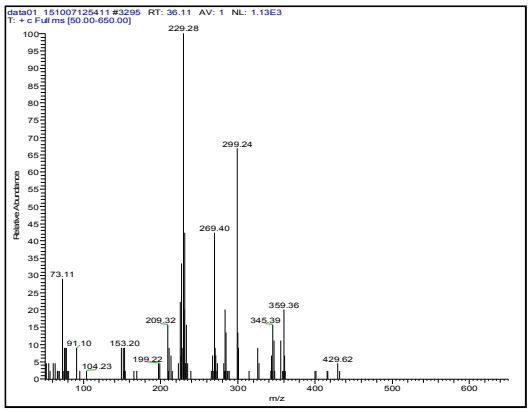

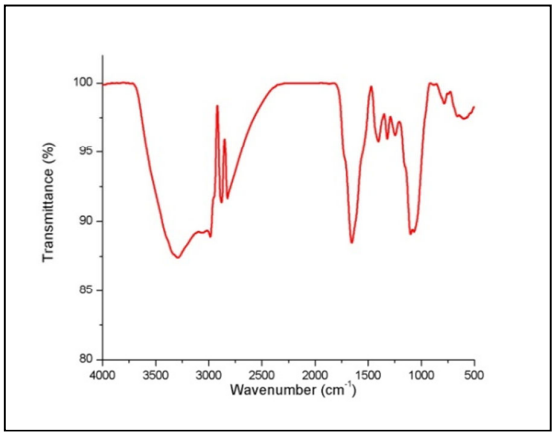

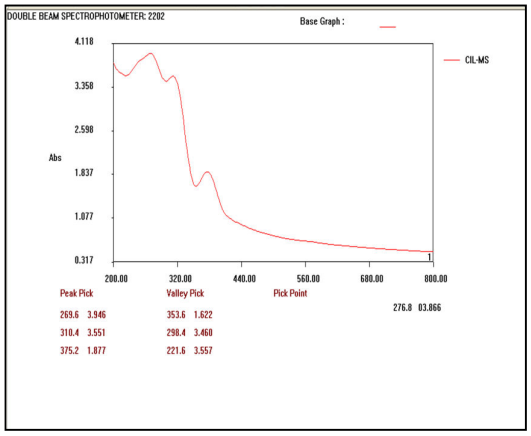

FTIR **UV**

Figure 4.12: Characterization of CIL extract

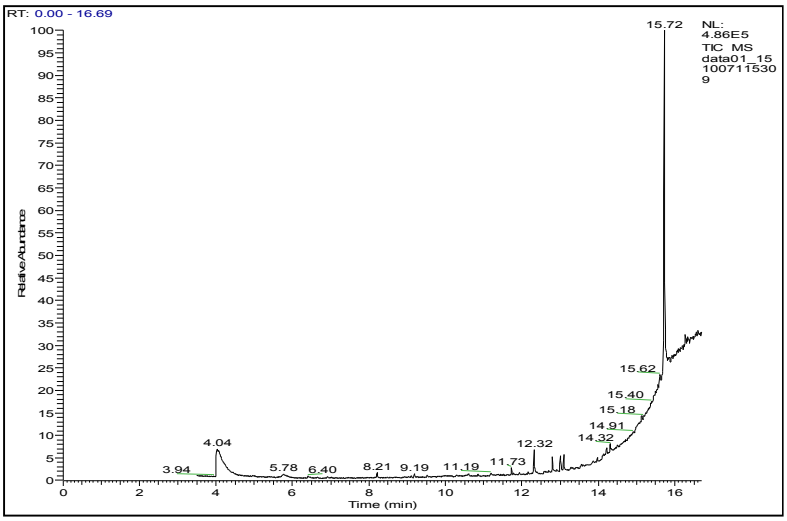

GC-MS

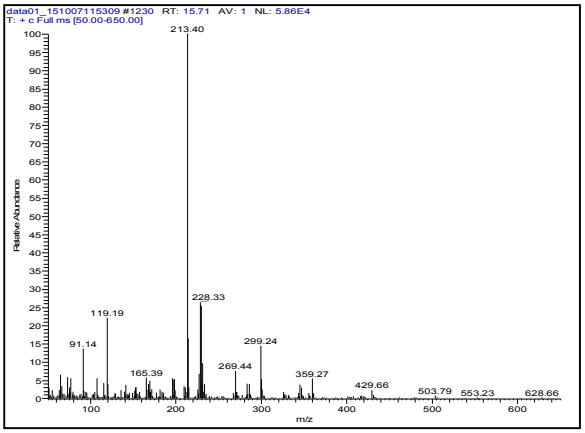

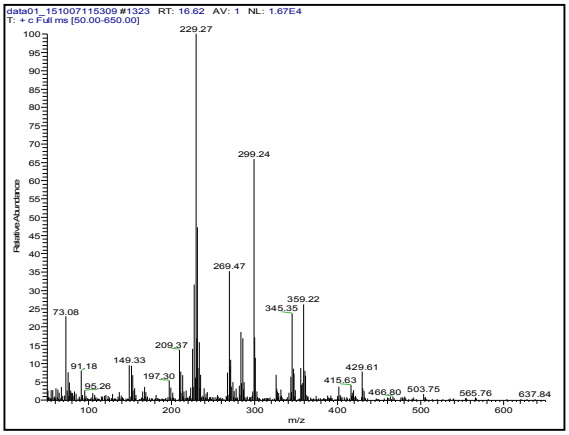

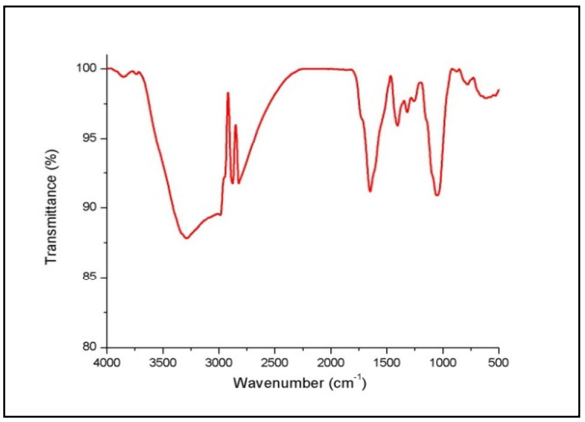

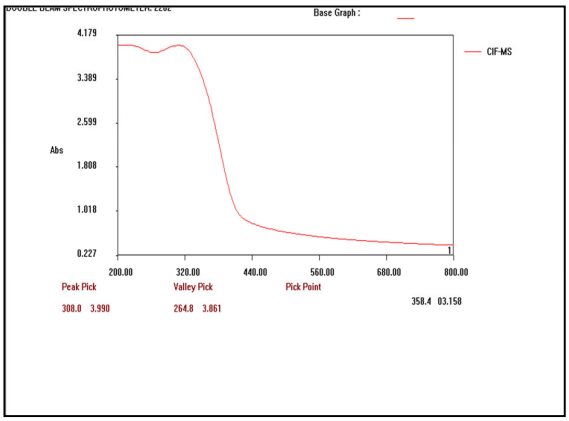

FTIR **UV**

Fig 4.13 : Characterization of CIF extract